DOPPLER EFFECT COMPENSATION FOR CYCLIC-PREFIX-FREE OFDM SIGNALS IN FAST-VARYING UNDERWATER ACOUSTIC CHANNEL

Y. V. Zakharov Department of Electronics, University of York, York, UK
A. K. Morozov Department of Applied Ocean Physics and Engineering, Woods Hole Oceanographic Institution, Woods Hole, USA
J. C. Preisig Department of Applied Ocean Physics and Engineering, Woods Hole Oceanographic Institution, Woods Hole, USA

Abstract

In this paper, we propose a receiver of OFDM signals in fast-varying multipath underwater acoustic channels with Doppler spread covering several subcarrier intervals. The OFDM signals are cyclic-prefix-free and the transmitted and pilot data are superimposed. The data symbols are encoded across subcarriers to exploit the frequency diversity. The receiver employs three stages for compensating the Doppler effect. The first stage deals with an average (over multipaths) time-varying compression factor and is implemented via time-varying re-sampling of the received signal. For the Doppler estimation, coarse and fine steps are proposed based on computation of the ambiguity function. The second stage compensates for the non-uniform Doppler distortion of multipath components and also deals with the multipath interference by exploiting a time-varying channel-estimate based equalizer with local spline interpolation of the equalizer weights. The third stage deals with the residual Doppler effect and it is implemented using a frequency-domain Doppler equalizer. The proposed receiver possesses a relatively low complexity as most of the operations are based on fast Fourier transform (FFT) and local spline interpolation. The receiver is verified using data obtained in a deep water experiment with data transmission at a distance of 40 km with a transducer towed by a surface vessel moving at a speed of 12 knots and continuously transmitting 1024-subcarrier OFDM symbols. The transducer had a complicated trajectory caused by the towing mechanism, which resulted in a severe time-varying Doppler distortion of the received signal. The acoustic signal was received by a single hydrophone. The performance of the receiver is investigated for different parameter settings. The results demonstrate that, in this experiment, the proposed receiver has allowed error-free detection at a data rate of 0.5 bits/s/Hz.

Index Terms - Doppler effect, OFDM, fast varying channel, experimental data, underwater acoustic communications

1 Introduction

High data-rate underwater acoustic communication attracts significant interest and OFDM transmission is considered as a promising technology for this purpose [1–3]. It can be efficiently combined with multi-antenna receivers and transmitters [4,5], thus improving the system performance. However, multi-antenna systems are not always available and can be complicated for underwater installation. Therefore, it is beneficial sometimes to deal with single-antenna transmitters and single-antenna receivers, even if this requires complicated signal processing, which nowadays becomes more affordable. It has been recognized that the severe double selectivity of the underwater acoustic channel introduces the main challenge in providing reliable communications [1, 2].

In this paper, we propose an OFDM communication system with single-transmit and single-receive antennas. The transmitted OFDM signal does not contain any guard interval and thus allows a high spectral efficiency to be achieved. Due to the zero guard interval, a superimposed pilot signal becomes periodic that greatly simplifies the processing in the receiver. The receiver is capable of dealing with the resulted intersymbol and intercarrier interference to reach the high detection performance, which is verified using experimental data.

2 Transmitted signal

We consider transmission of OFDM symbols without any guard interval, e.g. such as cyclic prefix or zero-padding. Thus, the duration of the transmitted OFDM symbol is the same as the orthogonality interval. One transmitted OFDM symbol is given by

$$s(t) = A \sum_{k=0}^{N-1} \cos[\omega_k t + \phi(k)] \tag{1}$$

where N is the number of subcarriers, A is the signal amplitude, $\omega_k = 2\pi f_k$, $f_k = f_c - F/2 + k/T_s$, f_c is the central frequency, T_s is the symbol duration and $F = N/T_s$ - frequency bandwidth of the transmitted signal. In our experiment, $N = 1024$, $f_c = 3072$ Hz, $T_s = 1$ s, $F = 1024$ Hz, and the frequency step between subcarriers is 1 Hz. The sequence $\phi(k)$ defines the phase modulation of subcarriers: $\sqrt{2}\exp\{j\phi(k)\} = D(k) + jM_1(k)$, where $j = \sqrt{-1}$ and $M_1(k)$ is the spectrum of a pilot signal used by the receiver for channel estimation; $M_1(k)$ is a binary pseudo-random sequence. The sequence $D(k)$ represents encoded information data. The transmitted data are encoded across the subcarriers using a $1/2$-rate convolutional code. The sequences $M_1(k)$ and $D(k)$ are binary with values ± 1. Thus, the data rate is approximately 0.5 bits/s/Hz. The OFDM symbols are transmitted in a data block one-by-one. In total, a data block of 340 OFDM symbols was transmitted in the experiment. Thus, the duration of the data block is 340 s.

3 OFDM receiver

In this section, we provide details of the proposed receiver, which is briefly described as follows.

The time-varying Doppler compression factor of the received signal is estimated with a time step $T_{\text{est}} < T_s$, i.e. smaller than the duration of one OFDM symbol. This is necessary due to fast channel variations. The estimate is obtained by computing the cross-ambiguity function between the received and pilot signals on a 2D-grid of delay and compression factor and finding the maximum [3, 6]. The estimate is further rectified using parabolic interpolation as described in [7]. These discrete-time estimates with the time-step T_{est} are linearly interpolated to the signal sampling rate and used to compensate for the time-varying Doppler effect by resampling the signal with the interpolated compression factor. The signal is then transformed into a complex-envelope signal within the frequency range $[-512, +512]$ Hz.

A linear time-domain channel-estimate based FIR equalizer is applied to the complex-envelope signal. The main purpose of the equalizer is to compensate for different compression factors of different multipath components which are seen as different rates of the multipath delay variations. The equalizer is not expected to produce a perfect single-path equivalent signal at the output, but rather reduce the multipath delay spread to a length short enough to deal with by a frequency domain equalizer that follows. The channel estimation is based on computing cross-correlation between the pilot and complex-envelope signals and it is performed with the same time step T_{est} as the estimation of the Doppler compression factor. The equalized signal is then transformed into the frequency domain using the Fast Fourier Transform (FFT).

Finally, N_{turbo} turbo iterations ($N_{\text{turbo}} = 2$ in our case) are repeated, each performing frequency-domain channel estimation, phase correction, residual channel equalization, and residual Doppler equalization. After the last turbo iteration, soft-decision Viterbi decoding [8] is applied to the recovered symbols. Both the channel estimators are based on the basis expansion model (BEM) with complex exponentials in the frequency domain. The channel estimation for the frequency-domain equalizer uses both the pilot symbols and tentative estimates of information symbols.

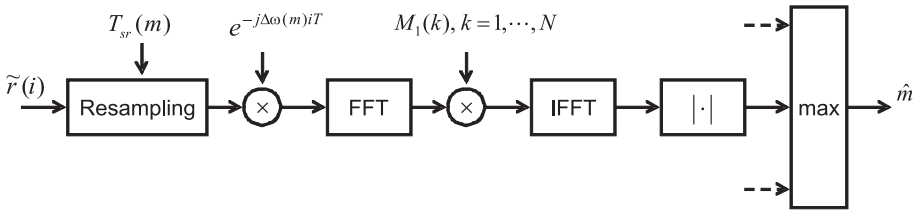

Figure 1: The coarse Doppler estimator. This scheme computes one section of the Doppler-delay ambiguity function. Maximum magnitude indicates the coarse Doppler estimate.

3.1 FRONT-END PROCESSING

The front-end processing includes analog band-pass filtering within the frequency band of the OFDM signal and analog-to-digital conversion with a sampling rate of $1/T = 12288$Hz. Then, the discrete-time signal is shifted in frequency towards zero frequency and, after a low-pass filtering, the spectrum of the signal is concentrated within the frequency range $[-512, +512]$ Hz. After the filtering we still keep the original sampling rate, which is high compared to the spectrum of the signal. This is required for further processing to achieve a low approximation error when resampling the signal in order to correct the Doppler distortions.

3.2 DOPPLER ESTIMATION

The Doppler estimation consists of two steps: coarse and fine estimation. The coarse estimation is based on the ambiguity function computed with a time step of $T_{\text{step}} < T_s$ using the pilot signal of $T_s = 1$ s length. The $\hat{m}$-th Doppler section with the maximum magnitude indicates the coarse Doppler estimate.

One Doppler section is computed as shown in Fig.1. The input signal $\tilde{r}(i)$ with the original sampling rate is resampled, downsampled and frequency shifted according to the mth compression factor $d(m) = (m - N_d - 1)\Delta d$, where $m = -N_d \dots N_d$, the parameter Δd defines the Doppler resolution, and $2N_d + 1$ is the number of Doppler sections. The sampling interval $T_{sr}(m)$ for the m-th Doppler section is given by $T_{sr}(m) = 12\, T/[1 + d(m)]$, where T is the original sampling interval and the coefficient 12 is the downsampling factor. The frequency shift is given by $\Delta\omega(m) = d(m)\ 2\pi f_c$, where f_c is the central frequency of the OFDM signal.

The resampling using the linear interpolation compensates for the time compression with the factor $1 + d(m)$. Note that the linear interpolation is applied to a signal with a frequency bandwidth of 512 Hz; with the original sampling frequency 12288Hz, the sampling factor is $12288/512 = 24$. According to [9], this sampling factor results in the interpolation error as low as about -50dB, i.e. the interpolation error can be ignored.

The time-compressed received signal now sampled at a rate of 1024Hz is correlated with the pilot signal by using the FFT of length $N = 1024$, multiplication by the pilot spectrum $M_1(k)$, and the inverse FFT (IFFT). The magnitude of the correlation function represents one (mth) section $A(k, m)$ of the ambiguity function, $k = 0, \dots, N - 1$. The maximum $\{\hat{k}, \hat{m}\} = \max_{m,k} |A(k, m)|$ provides the coarse estimate of the Doppler estimate.

The coarse Doppler estimate is further refined using parabolic interpolation. Specifically, the fine Doppler estimate is obtained as follows [7]: $\hat{d} = (I_3 - I_1)/[I_2 - (I_1 + I_3)/2]$, where $I_1 = |A(\hat{k}, \hat{m} - 1)|$, $I_2 = |A(\hat{k}, \hat{m})|$, and $I_3 = |A(\hat{k}, \hat{m} + 1)|$.

3.3 TIME-VARYING RESAMPLING

The fine Doppler estimate $\hat{d}$ is used for resampling the signal with a time varying compression factor obtained using linear interpolation of the estimates. This is indicated by the block *Resampling* in Fig. 2.

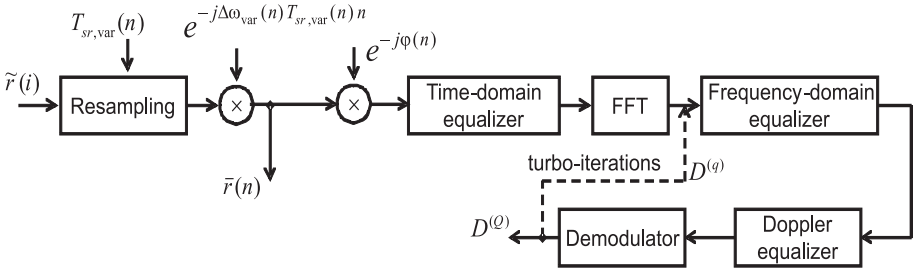

Figure 2: Time-varying resampling, time-varying linear equalization, frequency-domain equalization, and turbo processing.

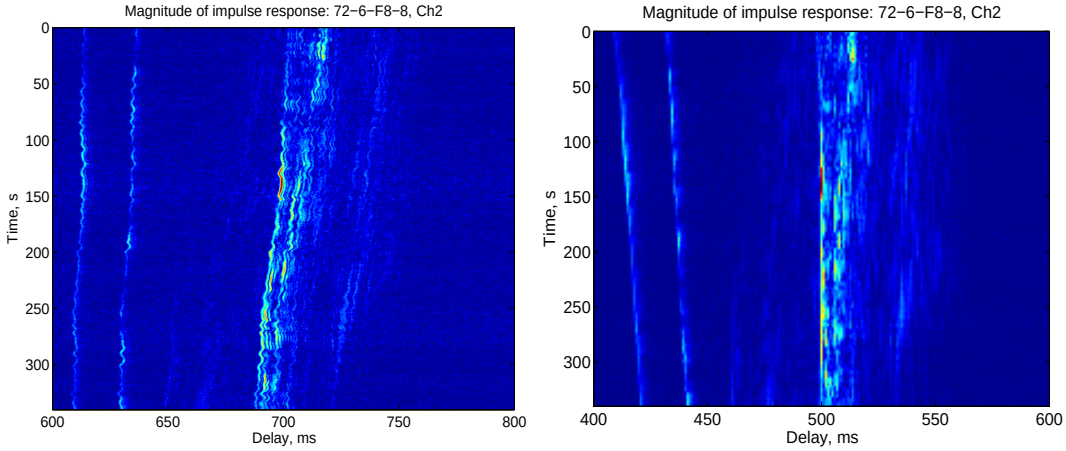

Figure 3: Impulse response variations before (left) and after (right) the time-varying resampling.

The resampling period $T_{sr,var}(n)$ and corresponding frequency shift $\Delta\omega_{var}(n)$ are computed similarly to that in the Doppler estimator, but taking into account the fact that we are using oversampling with a factor $N_\tau = 2$.

The effect of the resampling can be seen in Fig. 3, where estimates of the channel impulse response are shown before and after the resampling over the whole data block transmitted in the experiment. Although, the Doppler distortions after the resampling are significantly reduced, the Doppler correction does not allow complete compensation of the Doppler effect since different multipaths experienced different compression factors in the channel. This is well seen in Fig.3 where the first (in delay) two multipath clusters still have time-varying delays. However, as the delay variations are much slower now, this allows the use of a time-domain linear equalizer (see Fig. 2) to further improve the signal estimate by compensating for the residual time-delay variations.

3.3.1 Linear time-domain equalizer

The main tasks of the time-domain equalizer is to compensate for differently time-varying multipath delays and reduce the length of the channel time spread. The residual frequency selectivity can then be removed by the frequency domain equalizer as shown in Fig. 2. Prior to the linear equalization, the signal undergoes a phase correction by a value ϕ. The phase shift is computed as $\phi = \arg\{\hat{\mathbf{h}}_{\text{past}}^H \hat{\mathbf{h}}_0\}$ where $\hat{\mathbf{h}}_{\text{past}}$ and $\hat{\mathbf{h}}_0$ are past and present channel estimates, respectively.

Fig.4 shows the channel estimator used for computation of the time-domain equalizer. The frequency response estimation is based on the Basis Expansion Model, specifically, on approximation of the frequency response by orthogonal complex exponentials corresponding to different channel delays. The selection of the delays (and the basis functions for the approximation, or multipath selection) is

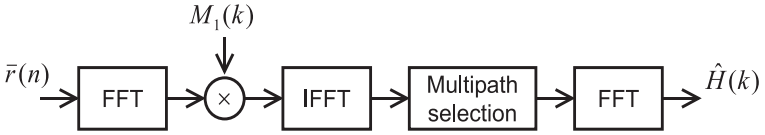

Figure 4: Channel estimator for the time-domain linear equalizer.

Figure 5: Computation of equalizer taps for the time-domain linear equalizer.

based on smoothing the instantaneous impulse response estimate obtained at the output of the IFFT block. This smoothed estimate is truncated based on the multipath spread and a number of multipath delays are chosen so that amplitudes of the smoothed response are higher than a threshold with respect to the maximum of the response. Specifically, if $\mathbf{h}_0$ is the smoothed response, then elements of the current channel estimate are given by

$$\hat{h}_{0,n} = \begin{cases} h_{0,n}, & \text{if } |h_{0,n}| > \gamma h_{\text{max}} \\ 0, & \text{otherwise} \end{cases} \tag{2}$$

where $h_{\text{max}} = \max_k |h_{0,k}|$ and γ is a small positive constant, $\gamma \in (0, 1)$. Finally, the FFT transforms the channel impulse response estimate into the frequency response estimate $\hat{H}(k)$, which is used for the MMSE equalization. The equalizer taps are computed as shown in Fig.5. The equalizer frequency response is then computed as $G(k) = \frac{\hat{H}^*(k)}{|\hat{H}(k)|^2+\sigma^2}$, where σ^2 is a small positive constant related to the noise level. The impulse response $g(n)$ of the equalizer is then computed using the inverse FFT of $G(k)$ and truncation to a required length L_{eq}.

The equalizer impulse response estimates $g(n)$ are obtained periodically with an interval T_{step}, which is chosen equal to the period of the Doppler estimation. The impulse response estimate is then converted into spline coefficients and further used for local cubic spline interpolation (see details on local spline interpolation in [9, 10]).

This processing is repeated N_τ times and produces N_τ equalized signals that are further combined in the frequency-domain equalizer.

3.3.2 Frequency-domain linear equalizer

The frequency-domain equalizer shown in Fig.2 is required to remove the residual time spread in the signal remaining after the time-domain equalization. In the first turbo iteration, estimation of the channel frequency response and computation of the equalizer frequency response are similar to that for the time-domain equalizer. However, at further turbo iterations, there is a difference. Firstly, we treat the (frequency-domain) signal obtained after the tentative demodulation as an extra pilot signal. Thus, the estimation is now performed with respect to a recovered signal that not only includes the pilot signal $M_1(k)$ but also a result of tentative demodulation $D^{(q)}(k)$ of the data symbols at all subcarriers. The index q relates to the qth turbo iteration, $q = 1, \ldots, Q$, that includes: frequency response estimation, equalization of the channel frequency response, Doppler equalization, and tentative demodulation. In our case, we use $Q = 2$. Secondly, the equalizer also combines $N_\tau = 2$ diversity channels obtained due to oversampling the signal (see description of the time-domain equalizer, Fig. 2).

3.3.3 Doppler equalizer

To deal with the residual Doppler spread still present in the signal, we use a Doppler equalizer. This equalizer is based on RLS adaptive filtering across the subcarriers with the pilot spectrum being the desired signal. The RLS filter has L_d taps (i.e., it combines L_d subcarriers) and the forgetting factor is $\lambda = 0.995$. Some details on this approach can be found in [11] and [6].

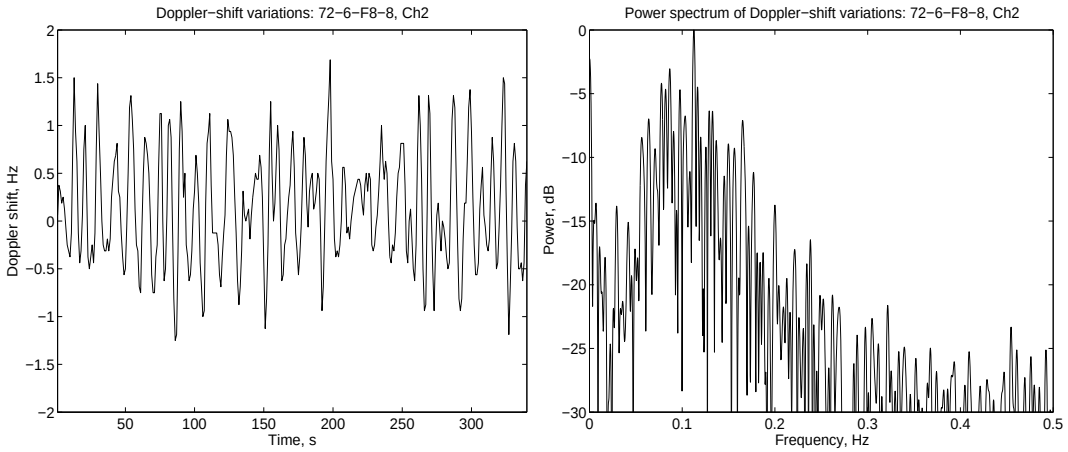

Figure 6: Doppler shift fluctuations over the data block (left) and their power spectrum (right) in the experiment.

3.3.4 Demodulation and decoding

For the tentative demodulation, we compare the real part of a subcarrier complex amplitude with a threshold η ($\eta = 0.05$). If the real part is positive and exceeds the threshold, we set the tentative demodulation result to $+1$; if it is negative and below the value $-\eta$, we set it to -1. Otherwise, the result of the tentative demodulation is set to 0. After completing Q iterations, the final result $D^{(Q)}$ (without the thresholding) is used as a soft input to the Viterbi decoder.

4 Ocean experiment

An acoustic source was towed by a ship moving towards the receiver at a speed of 6 m/s and depth of 200 m. Another (drifting) ship used an omnidirectional hydrophone positioned at a nominal depth of 400 m to record the received signal. The distance between the transmitter and receiver varied from 42 km to 40 km. The experiment took part in the Pacific Ocean in November 1989. See further details about the experiment in [12].

During the experiment, the wind speed was about 7-8m/s. The relatively fast speed of the transmitting vessel and high wind speed (high surface waves) have resulted in complicated movement of the towed transducer, and consequently to a complicated Doppler effect in the received acoustic signal. Fig.6 shows that the Doppler shift (and, consequently, the time compression factor) is fast varying in time (see also the left part of Fig. 3). Note that the variations shown in Fig.6 are obtained after compensation for the average Doppler shift due to the transducer movement at a speed of 12 knots. The spectrum of these fluctuations indicates a high power in the frequency interval between 0.05Hz and 0.2Hz. This corresponds to a typical time spectrum of surface waves; thus, the fluctuations of the Doppler shift are related to the surface waves. The range of the frequency Doppler shift, about ± 1.5 Hz, covers about three OFDM subcarriers, whereas, for reliable data detection, the final frequency error is known to be smaller than a few percents of the subcarrier interval.

Table 1 presents Bit-Error-Ratio (BER) performance of the receiver when applied to the experimental data. We consider several configurations of the receiver, including the full receiver as described above, and the receiver without some processing units to demonstrate their importance. We use three convolutional codes described by their polynomials in octal. In addition, Table 1 shows the BER performance of an ideal receiver in a perfectly known multipath channel without Doppler distortions; besides, there is no superimposed pilot and there is a cyclic prefix that perfectly removes the intersymbol interference.

Receiver configuration	Code [3 7]	Code [23 35]	Code [561 753]
1. Full receiver	$3 \cdot 10^{-4}$	0	0
2. No oversampling ($N_\tau = 1$)	$6 \cdot 10^{-4}$	$6 \cdot 10^{-5}$	$6 \cdot 10^{-5}$
3. No fine Doppler estimation	$3 \cdot 10^{-4}$	0	$1 \cdot 10^{-5}$
4. No cubic splines	$5 \cdot 10^{-4}$	$6 \cdot 10^{-6}$	$1 \cdot 10^{-5}$
5. No turbo iterations	$4 \cdot 10^{-4}$	$6 \cdot 10^{-6}$	$1 \cdot 10^{-5}$
6. No phase correction	$3 \cdot 10^{-4}$	$5 \cdot 10^{-5}$	$4 \cdot 10^{-5}$
7. Not accurate equalizer delay	$1 \cdot 10^{-3}$	$2 \cdot 10^{-4}$	$1 \cdot 10^{-4}$
1. Ideal receiver, SNR = 22 dB	$2 \cdot 10^{-5}$	0	0
2. Ideal receiver, SNR = 20 dB	$5 \cdot 10^{-5}$	$4 \cdot 10^{-7}$	$2 \cdot 10^{-7}$
3. Ideal receiver, SNR = 18 dB	$1 \cdot 10^{-4}$	$2 \cdot 10^{-6}$	$1 \cdot 10^{-6}$
4. Ideal receiver, SNR = 16 dB	$3 \cdot 10^{-4}$	$4 \cdot 10^{-6}$	$2 \cdot 10^{-6}$

Table 1: BER performance for different receiver configurations

Parameters of the full receiver are as follows. The ambiguity function is represented by $(2N_d+1) = 49$ Doppler sections with a frequency resolution of 0.125 Hz, i.e. 1/8 of the subcarrier interval. The length of the time-domain equalizer impulse response is 0.5 s, which is approximately three times longer than the channel multipath spread. The Doppler equalizer has $L_d = 5$ taps.

The presented results demonstrate that the BER performance of the full receiver is comparable to that of the ideal receiver at worst at SNR = 16 dB. The SNR in the experiment slightly varies over the transmitted data block and on average is 22 dB. Thus, our receiver loses in the performance to the ideal receiver less than 6 dB.

The results also show that the oversampling and phase correction provide significant improvement to the detection performance. The accurate equalizer delay with respect to the time window of the channel estimation is very important; the comparison is for the case of an extra delay of 0.25 s. The cubic spline interpolation (compared to zero-order interpolation) and turbo iterations are also important; without them the zero error transmission is not possible. The fine Doppler estimation does not look that important; however, it allows reduction in the frequency resolution when computing the ambiguity function without loosing in performance, and thus reducing the complexity.

Analysis of the complexity of the receiver shows that the highest contribution to the complexity come from the computation of the ambiguity function and spline interpolation of the equalizer impulse response. Most of the other processing benefits from using the FFT. In total, the receiver requires approximately 70 MFlops.

5 Conclusions

In this paper, we have proposed an iterative receiver that has allowed an error-free data transmission from a fast moving transducer to a single-phone receiver in a 40 km long underwater acoustic channel. The transmission based on prefix-free OFDM signals exploits $1/2$-rate convolutional coding across the subcarriers. Thus, a data rate of about 0.5 bs/Hz is achieved.

References

1. B. Li, S. Zhou, M. Stojanovic, L. Freitag, and P. Willett. Multicarrier communication over underwater acoustic channels with nonuniform Doppler shifts. *IEEE Journal of Oceanic Engineering*, 33(2): pp. 198–209, 2008.

2. C. R. Berger, S. Zhou, J. C. Preisig, and P. Willett. Sparse channel estimation for multicarrier underwater acoustic communication: From subspace methods to compressed sensing. *IEEE Transactions on Signal Processing*, 58(3): pp. 663–688, March 2009.

3. Y. V. Zakharov and V. P. Kodanev. Multipath-Doppler diversity of OFDM signals in an underwater acoustic channel. In *Proceedings IEEE Int. Conf. Acoustics, Speech, and Signal Processing. ICASSP'2000.*, vol. 5, pp. 2941–2944, 2000.

4. S. Roy, T. M. Duman, V. McDonald, and J. G. Proakis. High-rate communication for underwater acoustic channels using multiple transmitters and space–time coding: Receiver structures and experimental results. *IEEE Journal of Oceanic Engineering*, 32(3): pp. 663–688, 2007.

5. H. C. Song, W. S. Hodgkiss, W. A. Kuperman, T. Akal, and M. Stevenson. High-frequency acoustic communications achieving high bandwidth efficiency. *The Journal of the Acoustical Society of America*, 126: p. 561, 2009.

6. T. Eggen, A. Baggeroer, and J. Preisig. Communication over Doppler spread channels. Part I: Channel and receiver presentation. *IEEE Journal of Oceanic Engineering*, 25(1): pp. 62–71, 2000.

7. Y. V. Zakharov, V. M. Baronkin, and T. C. Tozer. DFT-based frequency estimators with narrow acquisition range. *IEE Proceedings Communications*, 148(1): pp. 1–7, 2001.

8. J. G. Proakis. *Digital communications*. McGraw-Hill, New York, 1995.

9. Y. V. Zakharov, T. C. Tozer, and J. F. Adlard. Polynomial spline-approximation of Clarke's model. *IEEE Trans. Signal Processing*, 52(5): pp. 1198–1208, May 2004.

10. Y. V. Zakharov and T. C. Tozer. Local spline approximation of time-varying channel model. *Electron. Lett.*, 37(23): pp. 1408–1409, 2001.

11. Z. Xu, Y. V. Zakharov, and V. P. Kodanev. Space-time signal processing of OFDM signals in fast-varying underwater acoustic channel. *OCEANS 2007-Europe*, : pp. 1–6, 2007.

12. C. Liu, Y. V. Zakharov, and T. Chen. Doubly-selective underwater acoustic channel model for moving transmitter/receiver. *IEEE Transactions on Vehicular Technology*, 61(3): pp. 938–950, 2012.